Journal Pre-proof

Rutile TiO_2 microwave dielectric ceramics prepared via cold sintering assisted two step sintering

Enda Zhao, Jianyu Hao, Xian Xue, Mingming Si, Jing Guo, Hong Wang

PII: S0955-2219(20)30978-X

DOI: https://doi.org/10.1016/j.jeurceramsoc.2020.12.009

Reference: JECS 13768

To appear in: *Journal of the European Ceramic Society*

Received Date: 14 October 2020

Revised Date: 7 December 2020

Accepted Date: 7 December 2020

Please cite this article as: Zhao E, Hao J, Xue X, Si M, Guo J, Wang H, Rutile TiO_2 microwave dielectric ceramics prepared via cold sintering assisted two step sintering, *Journal of the European Ceramic Society* (2020), doi: https://doi.org/10.1016/j.jeurceramsoc.2020.12.009

Rutile TiO_2 microwave dielectric ceramics prepared via cold sintering assisted two step sintering

Enda Zhao[1], Jianyu Hao[1], Xian Xue[1], Mingming Si[1], Jing Guo[1, *], Hong Wang[1, 2, 3*]

[1]*State Key Laboratory for Mechanical Behavior of Materials & School of Microelectronics, Xi'an Jiaotong University, Xi'an 710049, China*

[2]*Department of Materials Science and Engineering, Southern University of Science and Technology, Shenzhen 518055, China*

[3]*Shenzhen Engineering Research Center for Novel Electronic Information Materials and Devices, Southern University of Science and Technology, Shenzhen 518055, China*

**Corresponding author. E-mail: jingguo19@xjtu.edu.cn (J. Guo), wangh6@sustech.edu.cn (H. Wang)*

Abstract

In this work, a sintering route named cold sintering assisted two step sintering process (CSP-TS) is presented to prepare rutile TiO_2 ceramics with submicron grain sizes. Cold sintering process at 300 °C with tetrabutyl titanate and water as the liquid phase yields a 'green body' with a relatively high density of ~80%, and finally dense (98.5-99.8%) rutile TiO_2 ceramics with grain sizes of ~600 nm can be obtained in the second sintering process at 950-1000 °C. The microstructural analysis with SEM and TEM indicates that the CSP-TS samples sintered at 950 °C have an obvious phenomenon of recrystallization, accompanying by a decrease of amorphous phases and a formation of clear grain boundaries. Besides, the rutile TiO_2 ceramics prepared by CSP-TS possess excellent microwave dielectric properties with relative permittivity of 92.0-98.4 and Q×f values of 27,800-31,900 GHz. Therefore, it is feasible to utilize CSP-TS to prepare ceramics with small grain sizes at low sintering temperatures.

Keywords: *cold sintering process; rutile titanium dioxide; low-temperature sintering; microwave dielectric properties; submicron/nano-ceramics*

1. Introduction

Titanium dioxide (TiO_2) is one of the most widely used inorganic materials in a large number of applications such as pigments, cosmetics, electronics, photocatalysts, solar batteries, etc. It has three different crystalline phases including anatase, brookite, and rutile, and the anatase and brookite phase can convert to rutile phase irreversibly in a temperature range of 700-920 °C. [1] Among these three phases, the rutile phase is a wide bandgap semiconductor with excellent dielectric properties (high permittivity and low dielectric loss), making it promising in various electronic devices, such as high energy ceramic capacitors and varistors. [2, 3] Besides, due to the good microwave dielectric properties, TiO_2 ceramic is also widely applied in low-temperature co-fired ceramics (LTCC) technique and

functions in microwave passive components such as microwave filters and resonators [4-8]

Using traditional thermal sintering process, rutile TiO_2 can be densified well at a high temperature of 1400-1500 °C. [9-11] However, there will be oxygen vacancies formed with a part of Ti^{4+} reducing into Ti^{3+} during the sintering process in air or under low oxygen partial pressure, as Pullar et al. reported. [10] Because of the oxygen vacancies, rutile TiO_2 ceramic sintered at 1500 °C with a high density of over 98% shows a very low Q×f value of 6,000 GHz. [10] Sintering in oxygen atmosphere or using dopants such as Fe, Cr, Al, Cu, and Zn can resolve the problem of oxygen deficiency in the dense rutile TiO_2. [11] With the development of sintering techniques, new sintering processes such as microwave sintering, spark plasma sintering (SPS), hot press and flash sintering, have been proposed to study TiO_2 ceramics. [12-16] Thereinto, Marinel et al. reported that dense TiO_2 ceramics could be obtained by microwave sintering that could lower the sintering temperature by 150-175 °C comparing with traditional thermal sintering. [12] The TiO_2 ceramics prepared by microwave sintering at 1210 °C have the best microwave dielectric properties and show a Q×f value of 30,800 GHz, which is comparable to that of the traditional thermal sintered samples at 1300 °C (31,110 GHz). [12] Noh et al. used spark plasma sintering process in an oxygen atmosphere and obtained TiO_2 ceramics with a relative density of 99.1% at 760 °C. [13] The permittivity of TiO_2 prepared by SPS could reach 112.6, while the Q×f value is only 26,000 GHz. [13]

Cold sintering process (CSP) is a recently developed technique to densify ceramics and ceramic-based compositions. [17-20] The densification of the materials is realized through the none-equilibrium dissolution-precipitation process in transient solvents under a certain pressure. [18, 21] With cold sintering process, a lot of ceramic materials with high melting points can be sintered at ultra-low temperatures (< 350 °C). [17, 19, 22, 23] Recently, some microwave dielectric ceramics densified by CSP at a very low temperature (RT to 300 °C) have been reported, most of which are composed of some water-soluble materials [17, 24-28]. TiO_2, however, as an insoluble material in water and other common polar/non-polar solvents, has difficulty to be prepared by CSP. [29] Medri et al. have obtained nano-to-macroporous anatase TiO_2 with a relative density of 73% after CSP at 150 °C and post annealing at 500 °C. [29] They have also tried to utilize CSP to sinter anatase powders with 20% rutile, but the relative density is only 62%. [29] Very recently, Falk et al. have obtained nanograined TiO_2-Nb_2O_5 compacts with a relative density of above 91% after CSP at 200 °C, while the TiO_2 phase is still anatase from the XRD analysis. [30] To the best of our knowledge, although there are a number of researches involving low temperature sintering techniques to fabricate rutile TiO_2, no work on successfully densified rutile TiO_2 via CSP based sintering method has been published.

In this work, the cold sintering assisted two step sintering process (CSP-TS) was employed to

prepare rutile TiO_2, where a thermal sintering in the temperature range of 900-1000 °C was utilized after cold sintering process at 300 °C. The purpose of CSP is to prepare relatively dense 'green bodies' (~80%), so that highly dense rutile TiO_2 ceramics (>98%) could be obtained at a temperature much lower than that of traditionally thermal sintering. Another advantage of CSP is that the grain growth may be controlled at much lower temperatures, making it feasible to obtain rutile TiO_2 ceramics with small grain sizes (nano or submicron) via CSP-TS technique. [31] To augment the density of rutile TiO_2 ceramics during CSP, a mixture of tetrabutyl titanate ($Ti(OC_4H_9)_4$) and deionized water has been selected as the liquid phase. It is known that tetrabutyl titanate is typically used as one of the titania precursors during the hydrothermal synthesis of TiO_2 nanocrystallites. [32-35] It is also used to fabricate TiO_2 films via the sol-gel technique. Tetrabutyl titanate can hydrolyze rapidly, and the hydrolyzation process is described by the following equation:

$$Ti[OC_4H_9]_4 + xH_2O \rightarrow Ti[OC_4H_9]_{4-x}[OH]_x + xC_4H_9OH \quad (1)$$

Where x ranges from 1 to 4. The final product is $Ti(OH)_4$, and at a certain temperature it can be decomposed to amorphous or crystallite TiO_2 particles. To compare this sintering process with others, TiO_2 sintered at the same temperature but with traditional thermal sintering process was also studied. The microstructures, densities as well as microwave dielectric properties were investigated to characterize the rutile TiO_2 obtained in this study.

2. Experimental procedure

Fig. 1 presents the sample preparation procedures of rutile TiO_2 ceramics with different sintering routes. All the samples were prepared with highly pure rutile titanium dioxide nano powders (99.8%, Aladdin Biochemical Technology Co., Ltd, Shanghai, China, 25nm, rutile). Before sintering, the starting powders were dried at 100 °C for 24h. For cold sintering (CSP) and cold sintering assisted two step sintering (CSP-TS) samples, the powders were firstly mixed and homogenized with 16.7wt.% tetrabutyl titanate (≥98%, Sinopharm Chemical Reagent Co., Ltd, Shanghai, China) and 8.3wt.% deionized water using a mortar and a pestle. Then the mixtures were placing in a die at room temperature (RT), and the die was heated to 300 °C with a rate of 8-10 °C/min under the pressure of 350MPa. After holding the pressure at 300℃ for one hour, the mixtures were cold sintered into cylindrical samples (10mm in diameter and 5mm in thickness). At last, the samples were annealed at 300 °C for 4h to remove the possible water and organics. In the case of CSP-TS samples, the cold sintered samples were firstly annealed at 700 °C for 2h with a heating rate of 2 °C/min, and then annealed at 850-1025 °C for 2h with a heating rate of 1 °C/min. For traditional thermal sintering (TTS) samples, the powders were mixed with 5wt% polyvinyl alcohol (PVA) binder and pressed into cylindrical pellets (10mm in diameter and 5mm in thickness) under a pressure of 350 MPa. After

pre-fired at 500 °C for 1h to expel the blinder, the pellets were annealed at 700 °C for 2h with a heating rate of 2 °C/min, and then annealed at 850-1025 °C for 2h with a heating rate of 1 °C/min, as the same procedure of CSP-TS samples. To separate the contribution of pressure and tetrabutyl titanate, some samples were mixed with the same proportion of tetrabutyle titanate as CSP-TS samples and were sintered using TTS process. However, these TTS samples with tetrabutyl titanate have very similar relative densities and microwave dielectric properties to the samples with PVA. In that case, the following results are only from TTS samples without tetrabutyl titanate.

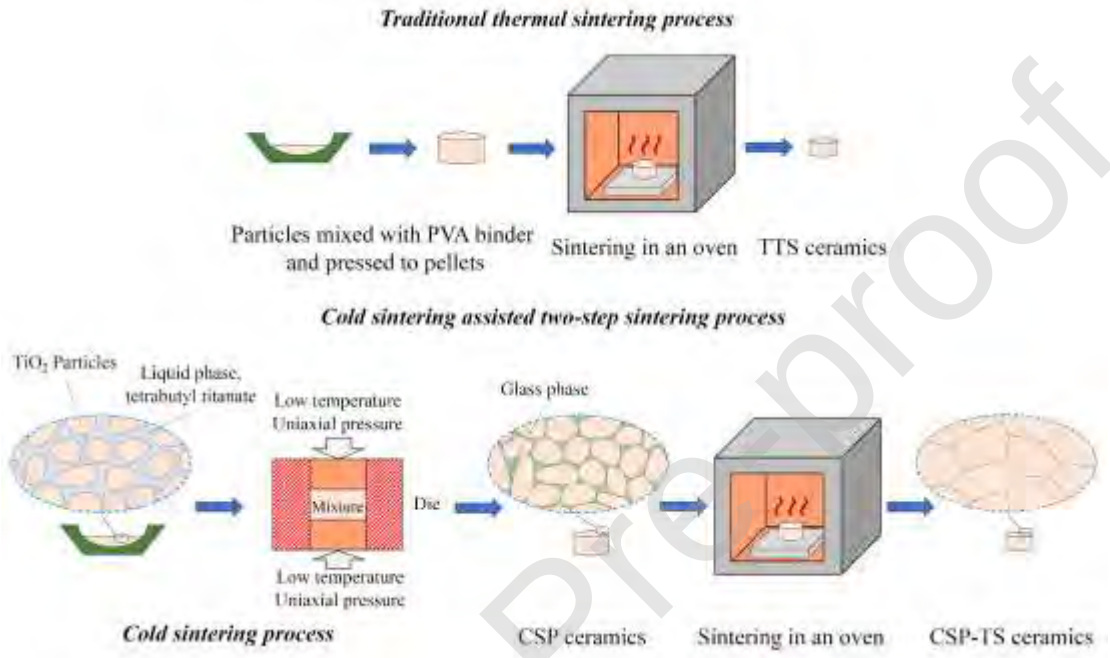

Fig. 1 Schematic illustrating the sintering procedures of rutile TiO_2 with cold sintering process (CSP), cold sintering assisted two step sintering (CSP-TS) and traditional thermal sintering (TTS)

The crystalline structures of staring powders and sintered samples were studied by X-ray diffraction (XRD) technique with Cu-*Kα* radiation (SHIMADZU XRD-7000, Tokyo, Japan). The wetted powder before CSP and CSP sample were studied by thermogravimetric analysis (TGA) with Synchronous Thermal Analyzer (NETZSCH STA 449F3, Selb, Germany), with a temperature range from RT to 700 °C by 10 °C/min in air. The microstructures were examined using scanning electron microscopes (SEM, Zeiss Gemini500, Carl Zeiss AG, Oberkochen, Germany and FEI QUANTA FEG 250, FEI, Hillsboro, Oregon, USA) and transmission electron microscope (TEM, JEOL JEM-F200 (HR), JEOL, Tokyo, Japan). The SEM images of CSP samples were obtained using the cross-sections of samples, and the SEM of CSP-TS and TTS samples were tested from polished and thermally etched samples. The surface of samples was polished by sandpapers and adamas polishing agent, and then the polished samples were annealed for 20 min at a temperature 150 °C lower than the sintering temperature. The specimens for TEM test were prepared using the focused iron beam (FIB, FEI Helios

NanoLab 600i, FEI, Hillsboro, Oregon, USA). The densities of samples were measured by Archimedes' method using ethanol as the liquid media. The dielectric properties at microwave frequencies were measured according to the $TE_{01\delta}$ shielded cavity method using a network analyzer (8720ES, Agilent, Palo Alto, CA) and a temperature chamber (Delta 9023, Delta Design, Poway, CA). The TCF values were measured in a temperature range of 25-85 °C and calculated by the following formula:

$$TCF = \frac{f_{85} - f_{25}}{(85-25) \times f_{25}} \times 10^6 \; ppm/°C \quad (2)$$

where the f_{25} and f_{85} are the $TE_{01\delta}$ resonant frequencies at 25 °C and 85 °C, respectively.

3. Results and discussion

Fig.2 represents the XRD patterns for the starting powder, and sintered samples with different sintering routes, including CSP at 300 °C, CSP-TS at 950 °C and TTS at 950 °C. For It is seen that all the diffraction peaks can be identified and indexed as the rutile TiO_2 structure according to the PDF card (PDF#21-1276), and no other phase can be detected. The full width at half maximum (FWHM) shows an obvious decrease from the raw powder and CSP samples to CSP-TS and TTS samples. For example, the FWHM values of (110) peak at 26-30º are 0.325 and 0.084 for CSP and CSP-TS samples, respectively. It is known that the grain size can be obtained from Scherrer formula using FWHM values. The calculated grain size for CSP samples is 28 nm, while the grain size for CSP-TS and TTS samples is over 100nm. Therefore, the grain growth of TiO_2 with a higher sintering temperature can be identified, which is further studied in the following microstructural analysis.

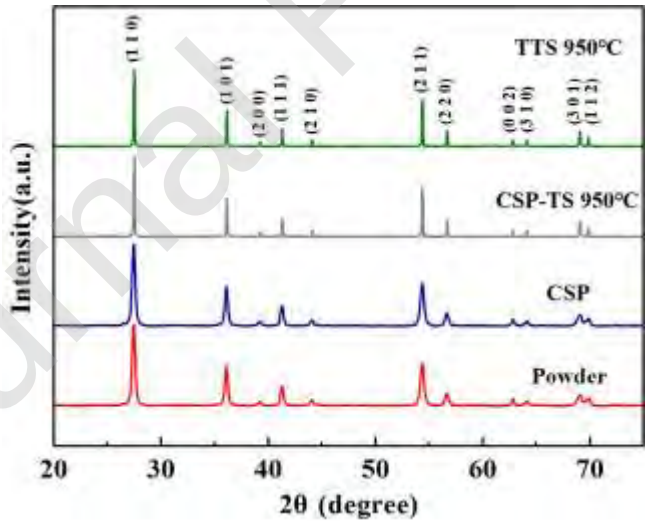

Fig. 2 XRD patterns of the starting powder and rutile TiO_2 ceramics prepared by CSP at 300 °C, CSP-TS at 950 °C and TTS at 950 °C

Fig.3 represents the TGA data of the wetted powder before CSP and the sample after CSP at 300 °C. The wetted powder is a mixture of TiO_2 powder, tetrabutyl titanate and deionized water (Details can be found in the experimental section). Tetrabutyl titanate is hydrolyzed with water, and the

generated $Ti(OH)_4$ precipitates on the surface of TiO_2 particles. As shown in Fig.3, the weight losses for both curves are slight because the content of tetrabutyl titanate and water is low. In the case of the wetted powder before CSP, there is a first drop of weight before 100 °C, a mild weight loss at 100-300 °C and another drop at 300-400 °C. The first drop of weight mainly results from the evaporation of water. The weight loss at 100-300 °C are mostly caused by the volatilization of butanol and the decomposition of partial $Ti(OH)_4$, and the drops at 300-400 °C are mainly caused by the decomposition of $Ti(OH)_4$. At 400-700 °C, there is nearly no change in weight, indicating that $Ti(OH)_4$ is completely decomposed to TiO_2 and there is no organic residual in the specimens. In the case of the sample after CSP, the weight loss before 300 °C is very slight and there is a slight drop of weight at 300-400 °C, which results from the decomposition of the $Ti(OH)_4$ residual. According to the TGA data, it is seen that $Ti(OH)_4$ generated from the hydrolyzation of tetrabutyl titanate can be partially decomposed to TiO_2 (Amorphous. Details can be found in the TEM results) during CSP at 300 °C, which precipitates on the surface of raw TiO_2 particles, aiding the densification of TiO_2. Finally, the $Ti(OH)_4$ residual can be completely decomposed in the second sintering process at 850-1025 °C and the amorphous TiO_2 is transformed to crystalline rutile TiO_2.

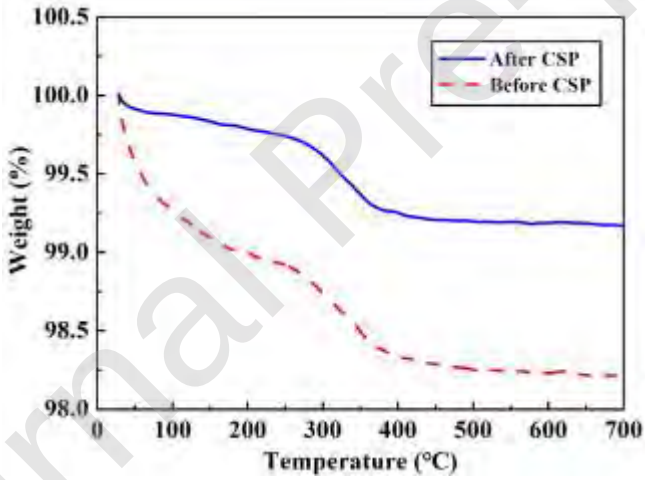

Fig. 3 Thermal gravimetric analysis (TGA) of wetted powder before CSP and sample after CSP at 300 °C

Fig.4 shows the SEM microstructures of specimens using CSP at 300 °C, CSP-TS at 900 °C and 950 °C, and TTS at 950 °C. As seen in Fig.4(a), the CSP sample has nanosized grains of ~25 nm with a small number of pores which is in consistent with the relative density of ~80%. After sintered at 900 °C, the grains grow from ~25 nm to ~270 nm, as shown in Fig.4(b) and (c). The phenomena of grain growth can also be observed in the CSP-TS samples sintered at 950 °C (Fig.4(d) and (e)) and TTS samples sintered at 950 °C (Fig.4(f)), which is in a good agreement with the analysis of FWHM of XRD data in the previous part. Only a few pores can be observed along the grain boundaries in the CSP-TS samples sintered at 900 °C, supporting a considerable increase in the relative density from ~80%

to 95%. In the Fig.4(d) and (e), the CSP-TS samples sintered at 950 °C have denser microstructures with a relative density of 98% and bigger grains with an average grain size of ~600 nm. When the sintering temperature is increased to over 1000 °C, abnormal grain growth and many pores can be clearly observed (Fig.S1 in Supporting Information), indicating a decrease in the relative density. In the Fig.4(f), the TTS samples sintered at 950 °C show a porous microstructure with a relative density of 85%. Comparing with CSP-TS samples sintered at the same temperature (950 °C), the grains size of TTS samples increase even further but with a much lower density, indicating that CSP-TS is a more efficient sintering method to densify rutile TiO_2 ceramics with smaller grain sizes.

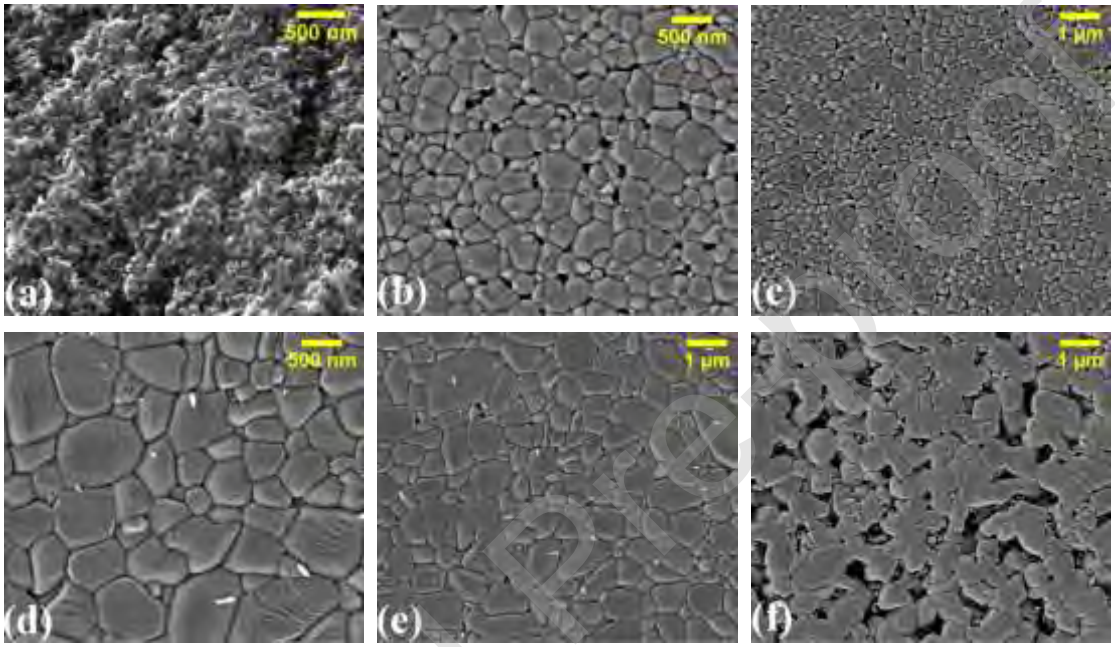

Fig. 4 SEM micrographs of the rutile TiO_2 ceramics, with (a) from the cross-section of samples and (b)-(f) from polished and thermally etched surface. (a) CSP samples cold sintered at 300 °C, (b)-(c) CSP-TS samples sintered at 900 °C, (d)-(e) CSP-TS samples sintered at 950 °C, and (f) TTS samples sintered at 950 °C

As shown in Fig.5, the details of microstructures of CSP and CSP-TS samples have been studied by high resolution TEM. Circular nanosized grains with a small amount of amorphous phases can be observed in the CSP samples (Fig.5(a-c)). Fig.5(c) shows a triple point of the grain boundaries, where a clear amorphous phase (arrowed) can be observed. The formation of amorphous phases mainly result from the decomposition of $Ti(OH)_4$ and dissolution-precipitation process during cold sintering process. At last, all the amorphous phases can be transformed to crystalline rutile TiO_2 during the second sintering process at a higher sintering temperature. In the Fig.5(d-f), the microstructure of CSP-TS samples sintered at 950 °C has a great change compared with CSP samples. Further densification and grain growth via the recrystallization occur during the sintering process at 950 °C. Circular grains with dozen nanometers transform to polygonal grains with several hundred nanometers (Fig.5(d)), which is

in a good agreement with the SEM analysis above. As seen in Fig.5(e) and (f), the amount of amorphous phases reduces, and clear grain boundaries can be observed after CSP-TS process.

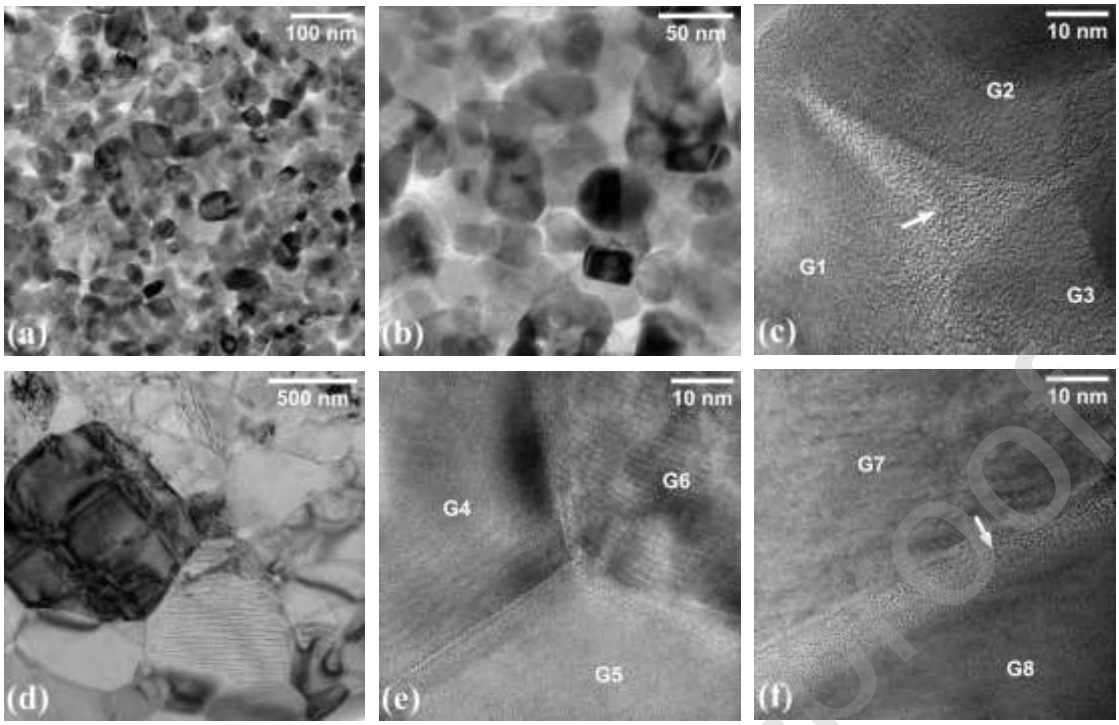

Fig. 5 TEM micrographs of the rutile TiO_2 ceramics. (a)-(c) CSP samples cold sintered at 300 °C, (d)-(f) CSP-TS samples sintered at 950 °C. Grains were individually numbered by G1-G8.

Fig.6 presents the relative densities and microwave dielectric properties of CSP-TS samples sintered in the temperature range of 850-1025 °C. As seen in Fig.6(a), the relative densities of CSP-TS samples increase first from 850 °C to 1000 °C with a maximum value of 99.8% at 1000 °C, and then appreciably decrease as the temperature continues to rise, which have been proved in the SEM results. In Fig.6(b), the relative permittivity increases from 83.0 to 100.3 with the sintering temperature increasing from 850 to 1025 °C. It is considered as a complex result of both densification and grain growths. The Q×f values show a trend similar to the density data, where a maximum value of 31,900 GHz can be obtained at 1000 °C, as seen in Fig.6(c). The drop of Q×f values at a higher sintering temperature (1025 °C) is similar to what Templeton et al. reported in their research [11], which might result from the oxygen vacancies. The TCF values show a slight change from 390 ppm/ °C to 440 ppm/ °C at the sintering temperature of 850-1025 °C (Fig.6(d)). From Fig.4-6, it is seen that CSP-TS samples sintered in the range of 950-1000 °C have high densities, excellent microwave dielectric properties, and small grain sizes (submicron) as well as homogeneous microstructures.

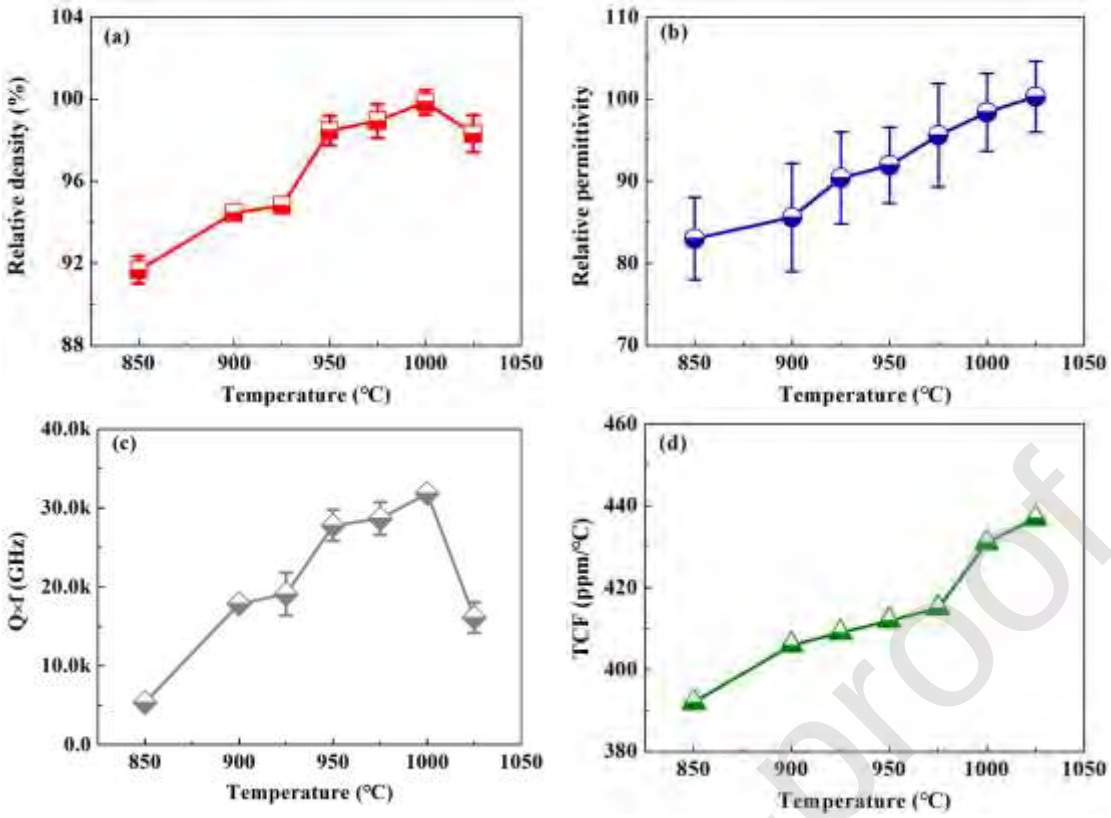

Fig. 6 Densities and microwave dielectric properties of CSP-TS rutile TiO_2 ceramics sintered at 850-1025 °C. (a) relative density, (b) relative permittivity, (c) Q×f, and (d) TCF.

Fig.7 summarizes the microwave dielectric properties of rutile TiO_2 sintered under different conditions. More detailed data are offered in Table.S1 in Supporting Information. In this work, for CSP-TS rutile TiO_2 samples sintered at 950-1000 °C, the permittivity Q×f, and TCF values are 92.0-98.4, 27,800-31,900 GHz, and 412-431 ppm/ °C, respectively. At the same sintering temperature of 950-1000 °C, the TTS samples show similar permittivity of 90.2-98.4 and TCF values of 430-440 ppm/ °C, but the Q×f values are much lower with only 2,600-7,800 GHz. From Fig.7, the TTS rutile TiO_2 samples can be well densified sintered at 1300-1500 °C, and the maximum permittivity of 106 and Q×f value of 46,500 GHz can be obtained at while sintered at 1400 °C. [10, 12, 36] The TiO_2 ceramics sintered at 1400 °C also have a very high TCF value of 465 ppm/ °C [36] While sintered at 1500 °C, the permittivity decreases to 96 and the Q×f value drastically decreases to 9,000 GHz because of the oxygen deficiency. [10] With 2wt% CuO addition,TiO_2 can be sintered well via TTS at 950 °C, and its permittivity is 102, similar to TTS samples at 1300-1400 °C. [37] However, the addition of CuO behaves as a second phase and affects the dielectric losses, so that the Q×f value of TiO_2 with 2wt% CuO is only 14,000 GHz. [37] The microwave sintering can only lower the sintering temperature to 1210 °C and obtain permittivity of 106 and a Q×f value of 30,800 GHz [12]. The spark plasma sintering in oxygen atmosphere can obtain dense TiO_2 ceramic at 760 °C with permittivity of 112.6 and a Q×f

value of 26,000 GHz [13], but it requires technical equipment and high cost. In summary, rutile TiO_2 ceramics can be well sintered using CSP-TS at 950-1000 °C and show good permittivity and Q×f values. With TTS, rutile TiO_2 needs to be sintered at high temperatures to obtain high permittivity and Q×f values. The addition of CuO can lower the sintering temperature of TiO_2, but it also deteriorates the Q×f values. In the LTCC technique, the ceramics need to be sintering under the melting point of certain co-fired metals (i.e. Cu: 1083 °C, Ag: 961 °C), and the sintering temperature of CSP-TS is as low as what the LTCC technique requires. Therefore, the cold sintering assisted two step sintering process is considered as a promising method to lower the sintering temperature of rutile TiO_2 ceramics as well as keeping good microwave dielectric properties, which is important for the application of TiO_2 in LTCC technique.

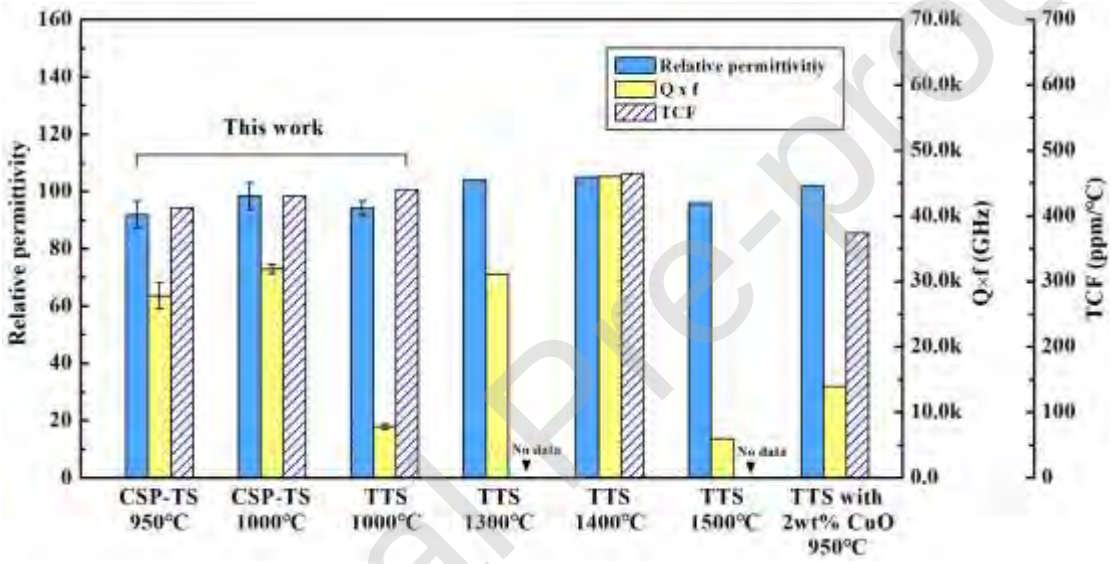

Fig. 7 Histogram comparing microwave dielectric properties of TiO_2 ceramics in this work with traditional thermal sintering (TTS) at 1300 °C [12], TTS at 1400 °C [36], TTS at 1500 °C [10] and TTS with 2wt% CuO at 950 °C [37].

4. Conclusion

In summary, this work introduces an improved sintering method based on cold sintering process to lower the sintering temperature of rutile TiO_2 which is called cold sintering assisted two step sintering. A relative density of ~80% can be obtained during the first sintering step (CSP at 300 °C) using tetrabutyl titanate as the liquid phase. After the second sintering step at 950-1000 °C in a furnace, rutile TiO_2 ceramics with submicron grain sizes (~600 nm) can be fully densified with relative densities of 98.5-99.8%. No impure phases can be observed for CSP and CSP-TS samples, and all the XRD peaks can be indexed as the rutile TiO_2 structure. The SEM and TEM results demonstrate that recrystallization and further densification occur in the second sintering step. Meanwhile, the rutile TiO_2

ceramics prepared by CSP-TS at 950-1000 °C show good microwave dielectric properties, with relative permittivity of 92.0-98.4 and Q×f values of 27,800-31,900 GHz. By contrast, the traditional thermal sintering cannot realize both the densification at a low temperature and good microwave dielectric properties at the same time. Therefore, cold sintering assisted two step sintering is a promising route to prepare rutile TiO_2 based ceramics applied in LTCC microwave devices. Furthermore, it is also feasible to obtain and study other dense ceramics with nano or submicron grain sizes using CSP-TS technique.

Declaration of interests

The authors declare that they have no known competing financial interests or personal relationships that could have appeared to influence the work reported in this paper.

Acknowledgments

The work was supported by the National Key Research Program (Grant No. 2017YFB0406303), National Natural Science Foundation of China (51902245) and Natural Science Foundation of Shaanxi Province China (2020JQ-044).

References

[1] D.A.H. Hanaor, C.C. Sorrell, Review of the anatase to rutile phase transformation, J. Mater. Sci. 46(4) (2011) 855-874.

[2] S.B. Cohn, Microwave bandpass filters containing high-Q dielectric resonators, IEEE Trans. Microw. Theory Tech. MT16(4) (1968) 218-227.

[3] M.F. Yan, W.W. Rhodes, Preparation and properties of TiO_2 varistors, Appl. Phys. Lett. 40(6) (1982) 536-537.

[4] L.-X. Pang, H. Wang, D. Zhou, X. Yao, Low-temperature sintering and microwave dielectric properties of TiO_2-based LTCC materials, J. Mater. Sci.-Mater. Electron. 21(12) (2010) 1285-1292.

[5] W. Wersing, Microwave ceramics for resonators and filters, Curr. Opin. Solid State Mat. Sci. 1(5) (1996) 715-731.

[6] M.F. Yan, W.W. Rhodes, Low-temperature sintering of TiO_2, Mater. Sci. Eng. 61(1) (1983) 59-66.

[7] M.T. Sebastian, H. Jantunen, Low loss dielectric materials for LTCC applications: a review, Int.

Mater. Rev. 53(2) (2008) 57-90.

[8] M.T. Sebastian, R. Ubic, H. Jantunen, Low-loss dielectric ceramic materials and their properties, Int. Mater. Rev. 60(7) (2015) 392-412.

[9] M.T. Sebastian, Chapter eleven - alumina, titania, ceria, silicate, tungstate and other materials, in: M.T. Sebastian (Ed.), Dielectric Materials for Wireless Communication, Elsevier, Amsterdam, 2008, pp. 379-443.

[10] R.C. Pullar, S.J. Penn, X. Wang, I.M. Reaney, N.M. Alford, Dielectric loss caused by oxygen vacancies in titania ceramics, J. Eur. Ceram. Soc. 29(3) (2009) 419-424.

[11] A. Templeton, X.R. Wang, S.J. Penn, S.J. Webb, L.F. Cohen, N.M. Alford, Microwave dielectric loss of titanium oxide, J. Am. Ceram. Soc. 83(1) (2000) 95-100.

[12] S. Marinel, D.H. Choi, R. Heuguet, D. Agrawal, M. Lanagan, Broadband dielectric characterization of TiO_2 ceramics sintered through microwave and conventional processes, Ceram. Int. 39(1) (2013) 299-306.

[13] J.H. Noh, H.S. Jung, J.-K. Lee, J.-R. Kim, K.S. Hong, Microwave dielectric properties of nanocrystalline TiO_2 prepared using spark plasma sintering, J. Eur. Ceram. Soc. 27(8-9) (2007) 2937-2940.

[14] S.C. Liao, K.D. Pae, W.E. Mayo, High pressure and low temperature sintering of bulk nanocrystalline TiO_2, Mater. Sci. Eng. A-Struct. Mater. Prop. Microstruct. Process. 204(1-2) (1995) 152-159.

[15] S.C. Liao, W.E. Mayo, K.D. Pae, Theory of high pressure low temperature sintering of bulk nanocrystalline TiO_2, Acta Mater. 45(10) (1997) 4027-4040.

[16] Y. Zhang, J. Nie, J. Luo, Effects of phase and doping on flash sintering of TiO_2, J. Ceram. Soc. Jpn. 124(4) (2016) 296-300.

[17] J. Guo, S.S. Berbano, H. Guo, A.L. Baker, M.T. Lanagan, C.A. Randall, Cold sintering process of composites: bridging the processing temperature gap of ceramic and polymer materials, Adv. Funct. Mater. 26(39) (2016) 7115-7121.

[18] J. Guo, R. Floyd, S. Lowum, J.-P. Maria, T.H. de Beauvoir, J.-H. Seo, C.A. Randall, Cold sintering: progress, challenges, and future opportunities, in: D.R. Clarke (Ed.), Annual Review of Materials Research, Vol 492019, pp. 275-295.

[19] J. Guo, H. Guo, A.L. Baker, M.T. Lanagan, E.R. Kupp, G.L. Messing, C.A. Randall, Cold sintering: a paradigm shift for processing and integration of ceramics, Angew. Chem.-Int. Edit. 55(38) (2016) 11457-11461.

[20] J. Guo, X. Zhao, T.H. De Beauvoir, J.-H. Seo, S.S. Berbano, A.L. Baker, C. Azina, C.A. Randall,

Recent progress in applications of the cold sintering process for ceramic-polymer composites Adv. Funct. Mater. 28(39) (2018) 180724.1-180724.15.

[21] J. Guo, A.L. Baker, H. Guo, M. Lanagan, C.A. Randall, Cold sintering process: A new era for ceramic packaging and microwave device development, J. Am. Ceram. Soc. 100(2) (2017) 669-677.

[22] J. Andrews, D. Button, I.M. Reaney, Advances in cold sintering, Johns. Matthey Technol. Rev. 64(2) (2020) 219-232.

[23] S. Grasso, M. Biesuz, L. Zoli, G. Taveri, A.I. Duff, D. Ke, A. Jiang, M.J. Reece, A review of cold sintering processes, Adv. Appl. Ceram. 119(3) (2020) 115-143.

[24] S.S. Faouri, A. Mostaed, J.S. Dean, D. Wang, D.C. Sinclair, S. Zhang, W.G. Whittow, Y. Vardaxoglou, I.M. Reaney, High quality factor cold sintered Li_2MoO_4-$BaFe_{12}O_{19}$ composites for microwave applications, Acta Mater. 166 (2019) 202-207.

[25] W.B. Hong, L. Li, H. Yan, X.M. Chen, Cold sintering and microwave dielectric properties of dense HBO_2-II ceramics, J. Am. Ceram. Soc. 102(10) (2019) 5934-5940.

[26] I.J. Induja, M.T. Sebastian, Microwave dielectric properties of mineral sillimanite obtained by conventional and cold sintering process, J. Eur. Ceram. Soc. 37(5) (2017) 2143-2147.

[27] M. Vaataja, H. Kahari, J. Juuti, H. Jantunen, Li_2MoO_4-based composite ceramics fabricated from temperature- and atmosphere-sensitive MnZn ferrite at room temperature, J. Am. Ceram. Soc. 100(8) (2017) 3626-3635.

[28] D. Wang, B. Siame, S. Zhang, G. Wang, X. Ju, J. Li, Z. Lu, Y. Vardaxoglou, W. Whittow, D. Cadman, S. Sun, D. Zhou, K. Song, I.M. Reaney, Direct integration of cold sintered, temperature-stable $Bi_2Mo_2O_9$-K_2MoO_4 ceramics on printed circuit boards for satellite navigation antennas, J. Eur. Ceram. Soc. 40(12) (2020) 4029-4034.

[29] V. Medri, F. Servadei, R. Bendoni, A.N. Murri, A. Vaccari, E. Landi, Nano-to-macroporous TiO_2 (anatase) by cold sintering process, J. Eur. Ceram. Soc. 39(7) (2019) 2453-2462.

[30] G.S. Falk, S. Yesid Gómez González, D. Hotza, Low-energy microwave synthesis and cold sintering of nanograined TiO_2-Nb_2O_5, Mater. Lett. 278 (2020) 128418.

[31] J. Hao, J. Guo, E. Zhao, M. Si, X. Yuan, F.-Z. Yao, H. Wang, Grain size effect on microwave dielectric properties of Na_2WO_4 ceramics prepared by cold sintering process, Ceram. Int. 46(17) (2020) 27193-27198.

[32] G. Wang, Hydrothermal synthesis and photocatalytic activity of nanocrystalline TiO_2 powders in ethanol-water mixed solutions, J. Mol. Catal. A-Chem. 274(1-2) (2007) 185-191.

[33] S. Pavasupree, J. Jitputti, S. Ngamsinlapasathian, S. Yoshikawa, Hydrothermal synthesis, characterization, photocatalytic activity and dye-sensitized solar cell performance of mesoporous

anatase TiO_2 nanopowders, Mater. Res. Bull. 43(1) (2008) 149-157.

[34] C.-h. Zhou, S. Xu, Y. Yang, B.-c. Yang, H. Hu, Z.-c. Quan, B. Sebo, B.-l. Chen, Q.-d. Tai, Z.-h. Sun, X.-z. Zhao, Titanium dioxide sols synthesized by hydrothermal methods using tetrabutyl titanate as starting material and the application in dye sensitized solar cells, Electrochim. Acta 56(11) (2011) 4308-4314.

[35] Q. Han, M. Yu, J. Liu, Nanocrystalline titanium dioxide prepared by hydrothermal method and its application in dye-sensitised solar cells, Micro Nano Lett. 8(5) (2013) 238-242.

[36] K. Fukuda, R. Kitoh, I. Awai, Microwave characteristics of TiO_2-Bi_2O_3 dielectric resonator, Jpn. J. Appl. Phys. 32(10) (1993) 4584-4588.

[37] D.W. Kim, B. Park, J.H. Chung, K.S. Hong, Mixture behavior and microwave dielectric properties in the low-fired TiO_2-CuO system, Jpn. J. Appl. Phys. 39(5A) (2000) 2696-2700.